



## Short communication

# Investigation of lithium carbide contamination in battery grade lithium metal

René Schmitz, Romek Müller, Steffen Krüger, Raphael W. Schmitz, Sascha Nowak, Stefano Passerini, Martin Winter<sup>\*\*</sup>, Christian Schreiner\*

Westfälische Wilhelms-Universität Münster, Institute of Physical Chemistry, MEET Battery Research Center, Corrensstrasse 46, 48149 Münster, Germany

## HIGHLIGHTS

- Lithium carbide has been found as impurity in battery grade lithium metal.
- Detection of  $\text{Li}_2\text{C}_2$  on the lithium surface and in the bulk material.
- Analysis by Raman spectroscopy, mass spectrometry, ICP-OES, and EDX.
- Discussion of possibilities for the source of contamination.

## ARTICLE INFO

### Article history:

Received 7 March 2012

Received in revised form

8 May 2012

Accepted 16 May 2012

Available online 5 June 2012

### Keywords:

Lithium metal

Lithium carbide

Impurity

Acetylene

Raman spectroscopy

Mass spectrometry

## ABSTRACT

Lithium carbide has been found as possible contamination in high purity lithium metal. Raman spectroscopy clearly shows its presence on the surface as well as in the bulk. Mass spectrometry revealed the formation of acetylene during hydrolysis of lithium metal also for the bulk material. The total lithium content of the lithium sample is determined with ICP-OES and the ratio of oxygen to carbon is investigated with EDX for the surface and the bulk. Possible sources of the lithium carbide contamination in battery grade lithium are discussed.

© 2012 Elsevier B.V. All rights reserved.

## 1. Introduction

Lithium metal is commonly used as anode material for commercial primary lithium batteries [1]. For the first secondary lithium batteries lithium metal was used as anode material as well until it was substituted by graphite because of its high safety hazards. It is well known that cycling of lithium metal anodes causes dendrite growth, which might result in a short circuit and thus a thermal runaway of the battery [2,3]. However, because of the high specific capacity of lithium metal anodes, lithium metal is still an attractive anode material for secondary lithium batteries, which is also used especially in combination with polymer electrolytes.[4] The theoretical capacity of a lithium metal electrode is

$3828 \text{ mAh g}^{-1}$ , 10 times higher than the capacity of graphite ( $372 \text{ mAh g}^{-1}$ ) which is the standard anode material in secondary lithium ion batteries [5]. Since for technical reasons a four times surplus of lithium metal would commonly be used, the practical specific anode capacity is reduced to about  $960 \text{ mAh g}^{-1}$ , this is still about 2.5 times higher than that of graphite [5]. Thus, investigation of lithium metal anodes is an interesting topic despite its challenges in terms of safety. The safety of lithium metal anodes is strongly determined by dendrite growth occurring upon battery cycling. The dendrite growth itself is influenced by the surface properties of the lithium metal anode and its Solid Electrolyte Interphase (SEI), respectively [6]. Impurities on the lithium metal anode surface might influence this SEI formation. High purity lithium metal for battery application is produced by fused salt electrolysis and purified by distillation [7,8] or by melting lithium metal at temperatures from  $400^\circ\text{C}$  to  $700^\circ\text{C}$  under vacuum [9]. The purity of commercially available battery grade lithium is usually specified as >99.9% (trace metals basis), but due to its high reactivity, Li is prone to be contaminated by impurities such as  $\text{Li}_2\text{O}$ ,  $\text{Li}_2\text{CO}_3$ , and

\* Corresponding author. Tel.: +49 251 83 36736; fax: +49 251 83 36032.

\*\* Corresponding author. Tel.: +49 251 83 36031; fax: +49 251 83 36032.

E-mail addresses: [martin.winter@uni-muenster.de](mailto:martin.winter@uni-muenster.de) (M. Winter), [chschreiner@gmx.net](mailto:chschreiner@gmx.net), [christian.schreiner@uni-muenster.de](mailto:christian.schreiner@uni-muenster.de) (C. Schreiner).

$\text{Li}_3\text{N}$ , which are formed by air contamination. In addition to these well known impurities,  $\text{Li}_2\text{C}_2$  has been found on the Li surface by Raman spectroscopy [10]. It was suggested that this  $\text{Li}_2\text{C}_2$  was formed due to  $\text{Li}_2\text{CO}_3$  decomposition caused by the Raman laser in the presence of lithium metal.

However, considering the known formation of stable hypervalent compounds of lithium with carbon (e.g.  $\text{Li}_3\text{C}$ ,  $\text{Li}_4\text{C}$  and  $\text{Li}_6\text{C}$ ) [11,12], it could be plausible that even sophisticated lithium purification procedures would not be sufficient to fully remove all carbon impurities. Mentioned hypervalent compounds were found to be stable in the gas phase and might lead to contamination of the purified lithium sample. Thus, as our investigations indicate, it could be possible that  $\text{Li}_2\text{C}_2$  is a common but hard to detect and thus also non-specified impurity in battery grade metallic lithium. In this work we investigated the presence of  $\text{Li}_2\text{C}_2$  impurities in battery grade lithium by Raman spectroscopy, mass spectrometry, and ICP-OES and EDX analysis.

## 2. Experimental

### 2.1. Materials

Lithium samples specified as battery grade in terms of purity were obtained from different commercial suppliers. Crystalline  $\text{Li}_2\text{C}_2$  was synthesized from the elements in a tantalum ampoule. A mixture of equal amounts of lithium metal and graphite were heated in an HF-oven at 1600 °C for 6 h. The purity of the crystalline  $\text{Li}_2\text{C}_2$  was proven by XRD analysis. The amorphization of part of the  $\text{Li}_2\text{C}_2$  was carried out with a ball mill (Frisch Pulverisette 7) in a tungsten carbide milling container with tungsten carbide balls. The synthesized crystalline  $\text{Li}_2\text{C}_2$  was ball milled for 10 min followed by a resting time of 2 min, which was repeated 10 times. The amorphization was confirmed by XRD, which did not show any diffraction pattern anymore after milling.

### 2.2. Raman spectroscopy

A Raman dispersive microscope (Bruker SENTERRA) was used to analyze the samples. The laser source was a green semiconductor laser with a wavelength of 532 nm and a laser power of 10 mW. A grating of 400 lines  $\text{mm}^{-1}$  was used as dispersive element and the aperture was a slit with a dimension of  $50 \times 1000 \mu\text{m}$ . A  $20\times$  objective was used for the microscope. All sample and cell preparations were carried out in an argon-filled glove box. The samples were measured in a sealed cell with a glass window ( $10 \mu\text{m}$  thickness, VWR). Ten integrations with an integration time of 1 s each were carried out to collect the spectra.

### 2.3. Mass spectrometry

A quadrupole mass spectrometer Prisma QMS 200 M (Pfeiffer Vacuum) recorded the mass to charge ratio ( $m/z$ ) signals. A flow meter red-y compact (Voegtlins Instruments) controlled the argon carrier gas flow to  $1.6 \text{ mL min}^{-1}$  through the sample chamber, which was connected by a stainless steel capillary to the online mass spectrometry cell. Millipore water, which was purged with argon to eliminate  $\text{CO}_2$  as possible carbon source was used for the hydrolysis reactions.

### 2.4. ICP-OES

The lithium sample was dissolved in methanol in an argon-filled glove box. A Spectro ARCOS ICP-OES (Spectro Analytical Instruments, Germany) instrument with axial plasma viewing was used for the element determination with a standard Fassel type torch

(No. 75160526, Spectro Analytical Instruments). For sample introduction, the system's peristaltic pump equipped with a cross flow nebulizer and a double-pass spray chamber (Scott type) was used. Lithium emission was detected at two individual emission lines simultaneously.

### 2.5. EDX

For the EDX measurements an in-house custom-made housing was used to transport the lithium under inert atmosphere from the glove box into the chamber of the SEM. The housing is equipped with a special mechanism, which opens the device under the low vacuum conditions in the SEM. The SEM was a Carl Zeiss Auriga equipped with an EDX from Oxford Instruments.

## 3. Results and discussion

### 3.1. Raman spectroscopy

In Fig. 1 the Raman spectra for untreated lithium metal (bottom) and synthesized crystalline  $\text{Li}_2\text{C}_2$  (top) are shown in the region of the typical  $\text{C}_2^{2-}$  vibration. It has already been reported by Naudin et al. that the mode at  $1845 \text{ cm}^{-1}$  was detected on untreated lithium [10]. In their studies it was proposed that the laser induces decomposition of  $\text{Li}_2\text{CO}_3$  present as surface impurity. In combination with elemental lithium the decomposition would lead to the reduction of  $\text{Li}_2\text{CO}_3$  and thus the formation of  $\text{Li}_2\text{C}_2$ , causing the mode at  $1845 \text{ cm}^{-1}$  from the symmetric stretching vibration of the carbon-carbon triple bond. The Raman shift of the acetylidy anion's symmetric stretching mode is found at around  $1877 \text{ cm}^{-1}$  for the synthesized  $\text{Li}_2\text{C}_2$  (cf. Fig. 1). Naudin et al. explained the shift by the amorphous structure of the  $\text{Li}_2\text{C}_2$  formed on lithium metal due to the laser impact [10].

To study the influence of amorphization on the  $\text{C}_2^{2-}$  vibration mode, an amorphous  $\text{Li}_2\text{C}_2$  sample was analyzed with the Raman spectrometer too. It can be seen that the Raman spectrum did not show any modes of the lattice phonons, which are normally present below  $500 \text{ cm}^{-1}$  for crystalline  $\text{Li}_2\text{C}_2$  (Fig. 2). This also proves, in addition to the XRD results, that the high-energy ball milling led to full amorphization of the  $\text{Li}_2\text{C}_2$ . However, the amorphization clearly did not cause any shift of the stretching vibration of the acetylidy anion. The amorphous sample showed a strong thermal emission though, which is the reason for the steep increase of the background signal with increasing wave numbers.

Thus, we suspect that the mode's shift to lower frequencies, i.e. the observed destabilization of the triple bond of the acetylidy

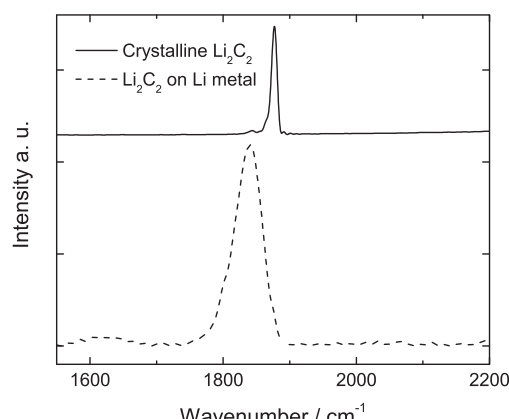
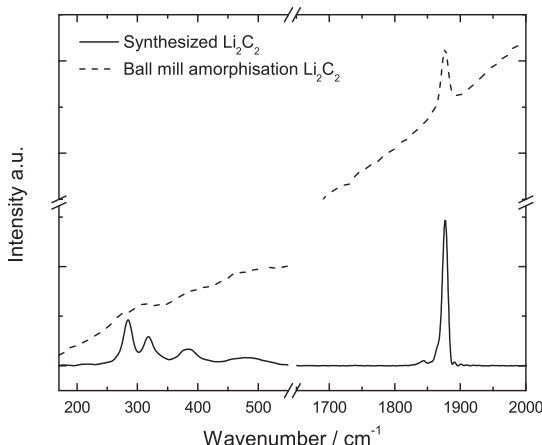


Fig. 1. Raman spectrum of synthesized  $\text{Li}_2\text{C}_2$  (top) and purchased lithium metal (bottom) in the region of the symmetric stretching vibration of the  $\text{C}_2^{2-}$  anion.



**Fig. 2.** Raman spectra of crystalline and the amorphous  $\text{Li}_2\text{C}_2$ .

anion, is caused by charge transfer from the lithium metal to the  $\text{Li}_2\text{C}_2$ . Using the molecular orbital theory for the  $\text{C}_2^{2-}$  anion, it can easily be seen that the acetylide anion's bonding orbitals are fully occupied. Thus, any negative charge transfer from the lithium metal to the acetylide anion would partially occupy anti-bonding molecular orbitals of the acetylide anion, causing destabilization of the triple bond and a shift of the vibrational band to lower wave numbers in the corresponding Raman spectrum. Thus, we propose that the mode at  $1845 \text{ cm}^{-1}$  can be assigned to the symmetric stretching of the acetylide anion triple bond, which is destabilized by charge transfer of electrons from the lithium metal.

To check the theory of laser-induced decomposition of  $\text{Li}_2\text{CO}_3$  present at the lithium surface as the source for  $\text{Li}_2\text{C}_2$ , we also investigated the bulk of the lithium metal by scraping the surface with a spatula in the glove box. If  $\text{Li}_2\text{C}_2$  was present on the surface only, one would not expect any acetylide Raman signal on the freshly exposed lithium metal surface. However, the fresh lithium metal surface gave the same signal at  $1845 \text{ cm}^{-1}$ , even with an intensity comparable to the surface. From this observation we concluded that the bulk of lithium metal seems to be contaminated with carbon containing impurities as well.

If the theory of Naudin et al. was correct this would imply that  $\text{Li}_2\text{CO}_3$  impurities were not only located on the surface (by contact to air traces) but also in the bulk. This seems being unlikely since lithium metal is synthesized form an eutectic melt of  $\text{LiCl}$  and  $\text{KCl}$  at  $400\text{--}460^\circ\text{C}$  and thus normally impurities of chloride were expected but not found. Traces of  $\text{Li}_2\text{CO}_3$  in  $\text{LiCl}$  are also unlikely because  $\text{LiCl}$  is normally obtained by the reaction of  $\text{HCl}$  with  $\text{Li}_2\text{CO}_3$ , which leads to the formation of gaseous  $\text{CO}_2$  and thus an elimination of  $\text{CO}_3^{2-}$ .[13]

Thus, based on our findings that  $\text{Li}_2\text{C}_2$  is not only located at the surface but also in the bulk of the lithium metal, we propose that  $\text{Li}_2\text{C}_2$  is already present in the lithium metal and not only formed from  $\text{Li}_2\text{CO}_3$  by the high laser energy applied for the Raman experiments. As already discussed bulk impurities of  $\text{Li}_2\text{CO}_3$  can be excluded because of the production procedure. In addition we showed that the amorphization of  $\text{Li}_2\text{C}_2$  does not cause the shift to lower frequencies, instead we propose that a charge transfer is responsible for the observed shift of the acetylide signal of  $\text{Li}_2\text{C}_2$  traces in lithium.

### 3.2. Mass spectrometry

To support our theory that  $\text{Li}_2\text{C}_2$  was not formed by the impact of the Raman laser, lithium metal samples were hydrolyzed in water to analyze the evolved gases by mass spectrometry. The

hydrolysis of  $\text{Li}_2\text{C}_2$  leads to the formation of gaseous acetylene that gives a signal at  $26 \text{ m/z}$ , which indicates the existence of  $\text{Li}_2\text{C}_2$  in the lithium metal sample without the impact of any laser light. To figure out whether the  $\text{Li}_2\text{C}_2$  is only located on the surface or also in the bulk of the lithium metal, partial hydrolysis was carried out by the addition of just a small amount of water to an excess of Li so that only part of the lithium metal was hydrolyzed. Then, by a subsequent second addition of water the remaining lithium metal after the first step was hydrolyzed and the evolved gases were detected again. With this experiment we were able to show that  $\text{Li}_2\text{C}_2$  impurities are also present in the bulk since all the  $\text{Li}_2\text{C}_2$  on the surface was already hydrolyzed during the first step. The mass signals of  $26 \text{ m/z}$  ( $\text{H}_2\text{C}_2$ ),  $18 \text{ m/z}$  ( $\text{H}_2\text{O}$ ) and  $2 \text{ m/z}$  ( $\text{H}_2$ ) are shown over time in Fig. 3. The signal of  $26 \text{ m/z}$  can be assigned to acetylene, which is formed and released by the reaction of lithium carbide with water, yielding acetylene and lithium hydroxide. The addition of water to lithium metal of course also leads to hydrogen formation and local heating which causes an increased water vapor release which could be seen by the water ( $18 \text{ m/z}$ ) and the hydrogen ( $2 \text{ m/z}$ ) signal count increase.

As a reference, the synthesized  $\text{Li}_2\text{C}_2$  showed a similar behavior upon injection of water into the reaction chamber. In this case, a change of the signals for  $26 \text{ m/z}$  and  $18 \text{ m/z}$  was detected as shown in Fig. 4. The signal of water ( $m/z = 18$ ) appears without a peak due to the less violent reaction, water vapor is stripped to the MS by the carrier gas flow.

### 3.3. ICP-OES and EDX

To estimate the lithium samples' purity, ICP-OES was used to determine the relative lithium content in a lithium sample. ICP-OES was also used to figure out whether any other impurities than carbon were present in the lithium metal. Since ICP-OES cannot be used to determine carbon or oxygen, EDX was used in addition. For the ICP-OES measurement a known amount of lithium metal was first dissolved in methanol in an argon-filled glove box and then further diluted with water. The ICP-OES analysis of the hydrolyzed lithium sample gave a lithium content of 99.1% by wt. Since there was no indication for the presence of any other elements as impurities, it could be concluded that the lithium sample may contain only carbon, oxygen, hydrogen, or nitrogen as possible impurities. The quantification of oxygen, carbon, and hydrogen is not possible by ICP-OES because of the used solvents water and methanol. For nitrogen an analysis is impossible since ambient air disturbs the measurement. To determine these elements, except hydrogen, EDX was carried out on scraped and unscraped lithium metal samples. The results are given in Table 1.

EDX showed no indications for the presence of any other elements than carbon and oxygen as possible impurities. A higher

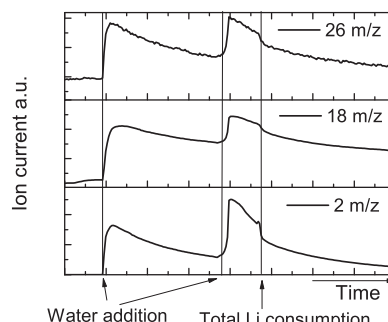


**Fig. 3.** Mass traces of acetylene, water, and hydrogen after the addition of water to untreated lithium metal.

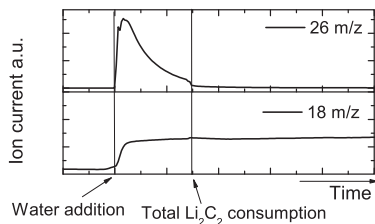


**Fig. 4.** Mass traces of acetylene and water after the addition of water to synthesized Li<sub>2</sub>C<sub>2</sub>.

**Table 1**

Relative atom contents of carbon and oxygen of scraped and unscraped lithium samples.

Sample	Relative carbon content (%)	Relative oxygen content (%)
Unscraped lithium (surface)	36	64
Scraped lithium (bulk)	60	40

amount of oxygen than carbon was detected for the unscraped sample while the content of carbon was higher than oxygen for the scraped sample. Since a native layer of Li<sub>2</sub>O and Li<sub>2</sub>CO<sub>3</sub> is always formed on lithium upon contact to air traces, it makes sense that the relative oxygen content was higher for the surface sample than for the scraped bulk sample which was only briefly exposed to the high purity argon atmosphere in the glove box. The detected relative carbon content on the scratched lithium metal is therefore another indication of bulk carbon impurities, which may result from the synthesis of the metallic lithium.

#### 4. Conclusion

We have shown by Raman spectroscopy, mass spectrometry, and EDX that Li<sub>2</sub>C<sub>2</sub> is present in commercial high purity battery grade lithium metal and that it can be found in the bulk material as well as on the surface. In literature it was reported that XPS measurements showed the presence of Li<sub>2</sub>C<sub>2</sub> after sputtering lithium metal [14], but in contrast to the theory of a laser-induced Li<sub>2</sub>CO<sub>3</sub> decomposition as origin of Li<sub>2</sub>C<sub>2</sub>, we suggest that the Li<sub>2</sub>C<sub>2</sub> is already present in lithium as an impurity, which is difficult to detect. Raman spectroscopy and mass spectrometry were useful tools to elucidate the presence of Li<sub>2</sub>C<sub>2</sub> in lithium. A possible source for such a contamination could be the fused salt electrolysis of lithium itself. Commonly used carbon cathodes for the fused salt electrolysis [15] most likely lead to the contamination of the lithium metal with Li<sub>2</sub>C<sub>2</sub> [16,17]. The alternative usage of mild steel as electrode material is a possible source for carbon contaminations as well [18]. The efficiency of lithium purification methods such as

distillation could be limited because lithium forms stable hypervalent molecules with many main group elements, which are stable in the gas phase. Especially the hypervalent carbon-based molecules are interesting with respect to the results shown in this paper. Lithium and carbon form compounds like Li<sub>3</sub>C, Li<sub>4</sub>C, and Li<sub>6</sub>C at temperatures around 700 °C in the gas phase [11,12]. This could explain why it is apparently so difficult to remove all carbon contaminations. The probably mostly unnoticed possible presence of Li<sub>2</sub>C<sub>2</sub> as an impurity in battery grade lithium metal therefore needs further attention because its impact on battery performance and cycling behavior in lithium metal cells is not clear yet. For example, lithium carbide could probably have an influence on SEI formation, either directly or indirectly by e.g. scavenging HF traces from LiPF<sub>6</sub> electrolytes.

#### Acknowledgments

The authors gratefully acknowledge the financial support of this work by the DFG (German Research Foundation) as part of the research initiative PAK 177 "Funktionsmaterialien und Materialanalytik zu Lithium-Hochleistungsbatteien" (contract numbers WI 2929/1-1 and WI 2929/5-1) on materials for lithium ion batteries.

#### References

- [1] J.O. Besenhard, Handbook of Battery Materials, Wiley-VCH, 1999.
- [2] C. Brissot, M. Rosso, J. Chazalviel, S. Lascaud, Journal of Power Sources 81 (1999) 925.
- [3] M. Rosso, C. Brissot, A. Teyssot, M. Dolle, L. Sannier, J.-M. Tarascon, R. Bouchetc, S. Lascaud, Electrochimica Acta 51 (2006) 5334.
- [4] [a] V. Di Noto, S. Lavina, G.A. Giffin, E. Negro, B. Scrosati, Electrochimica Acta 57 (2011) 4;  
[b] F.B. Dias, L. Plomp, J.B.J. Veldhuis, Journal of Power Sources 88 (2000) 169.
- [5] M. Winter, J.O. Besenhard, M.E. Spahr, P. Novak, Advanced Materials 10 (1998) 725.
- [6] Y. Sasaki, M. Hosoya, M. Handa, Journal of Power Sources 68 (1997) 492.
- [7] R.R. Rogers, G.E. Viens, Journal of the Electrochemical Society 98 (1951) 483.
- [8] P.H. Schmidt, Journal of the Electrochemical Society 113 (1966) 201.
- [9] Roumieu, R. Metaux Speciaux S.A.: United States, 1986.
- [10] C. Naudin, J.L. Bruneel, A. Chami, B. Desbat, J. Grondin, J.C. Lasseguès, L. Servant, Journal of Power Sources 124 (2003) 518.
- [11] A. Maercker, Angewandte Chemie-International Edition in English 31 (1992) 584.
- [12] H. Kudo, C.H. Wu, Journal of Nuclear Materials 201 (1993) 261.
- [13] U. Wielmann, R.J. Bauer, in: Ullmann's Encyclopedia of Industrial Chemistry, Wiley-VCH, 2007.
- [14] K. Kanamura, S. Shiraishi, H. Tamura, Z. Takehara, Journal of the Electrochemical Society 141 (1994) 2379.
- [15] J. Deberitz, Lithium, sv corporate media, 2006.
- [16] W.K. Hsu, J.P. Hare, M. Terrones, H.W. Kroto, D.R.M. Walton, P.J.F. Harris, Nature 377 (1995) 687.
- [17] W.K. Hsu, J. Li, H. Terrones, M. Terrones, N. Grobert, Y.Q. Zhu, S. Trasobares, J.P. Hare, C.J. Pickett, H.W. Kroto, D.R.M. Walton, Chemical Physics Letters 301 (1999) 159.
- [18] M.G. Barker, S.A. Frankham, Journal of Nuclear Materials 107 (1982) 218.